



Synthesis and phosphorescence properties of Mn^{4+} , La^{3+} and Ho^{3+} in $\text{MgAl}_2\text{Si}_2\text{O}_8$

Nilgun Ozpozan Kalaycioglu*, Esra Çırçır

Department of Chemistry, Faculty of Science, Erciyes University, Kayseri, 38039, Turkey

ARTICLE INFO

Article history:

Received 13 May 2011

Accepted 6 August 2011

Available online 2 September 2011

Keywords:

Mn^{4+}

La^{3+}

Ho^{3+}

$\text{MgAl}_2\text{Si}_2\text{O}_8$ phosphors

Aluminosilicates

ABSTRACT

Mn^{4+} , La^{3+} and Ho^{3+} doped $\text{MgAl}_2\text{Si}_2\text{O}_8$ -based phosphors were first synthesized by solid state reaction. They were characterized by thermogravimetry (TG), differential thermal analysis (DTA), X-ray powder diffraction (XRD), photoluminescence (PL) and scanning electron microscopy (SEM). The phosphors were obtained at about 1300 °C. They showed broad red and fuchsia-pink emission bands in the range of 610–715 nm and had a different maximum intensity when activated by UV illumination. Such a fuchsia-pink emission can be attributed to the intrinsic d–d transitions of Mn^{4+} .

© 2011 Elsevier B.V. All rights reserved.

1. Introduction

Luminescent materials with long afterglow are kinds of energy storage materials that can absorb both UV and visible light from the sun and gradually release this energy in the dark at a certain wavelength. These kinds of long lasting phosphors have been widely studied by many researchers [1–3].

Silicates therefore are suitable hosts for phosphors because of their high physical and chemical stability. The luminescence of rare earth ions in the silicate host has been studied for a long time. In recent years, silicate phosphors have been reported by researchers [4–13].

In this paper, $\text{MgAl}_2\text{Si}_2\text{O}_8$, $\text{MgAl}_2\text{Si}_2\text{O}_8:\text{Mn}^{4+}$, $\text{MgAl}_2\text{Si}_2\text{O}_8:\text{Mn}^{4+}$, La^{3+} and $\text{MgAl}_2\text{Si}_2\text{O}_8:\text{Mn}^{4+}$, Ho^{3+} were first synthesized by solid state reaction at 1300 °C. Their thermal behavior, crystal structure, photoluminescence properties and morphological characterization were then investigated.

2. Experimental

$\text{MgAl}_2\text{Si}_2\text{O}_8$, $\text{MgAl}_2\text{Si}_2\text{O}_8:\text{Mn}^{4+}$, $\text{MgAl}_2\text{Si}_2\text{O}_8:\text{Mn}^{4+}$, La^{3+} and $\text{MgAl}_2\text{Si}_2\text{O}_8:\text{Mn}^{4+}$, Ho^{3+} phosphors were synthesized using the solid state technique. All the starting materials, $4\text{MgCO}_3 \cdot \text{Mg}(\text{OH})_2 \cdot 5\text{H}_2\text{O}$ (A.R.), Al_2O_3 (99.0%), SiO_2 (99.8%), MnO_2 (99.0%), La_2O_3 (99.99%) and Ho_2O_3 (99.99%) were weighed according to the nominal compositions of $\text{MgAl}_2\text{Si}_2\text{O}_8$, $(\text{Mg}_{0.90}\text{Mn}_{0.10})\text{Al}_2\text{Si}_2\text{O}_8$, $(\text{Mg}_{0.88}\text{Mn}_{0.10}\text{La}_{0.02})\text{Al}_2\text{Si}_2\text{O}_8$ and $\text{Mg}_{0.88}\text{Mn}_{0.10}\text{Ho}_{0.02}\text{Al}_2\text{Si}_2\text{O}_8$. These powders were mixed homogeneously in an agate mortar for 3 h. Small quantities of H_3BO_3 (A.R. and 1 wt%) were added as a flux during the mixing. A small amount of sample was taken for thermal analysis (TG/DTA) to study the phase-forming process. Thermogravimetry (TG) and differential thermal analysis (DTA) were carried out by using a DTA/TG system (Perkin

Elmer Diamond type). The samples were heated at a rate of 10 °C min^{−1} from room temperature to 1300 °C.

Afterwards the sintering conditions of the phosphors, including the pre-firing temperature and synthesizing temperature, were determined in two steps: firstly, the mixtures were pre-fired at 900 °C for 3 h in a porcelain crucible in air, and secondly the pre-fired samples were sintered at 1300 °C for 3 h in air, in a porcelain crucible. After these procedures the phosphors were obtained and their crystal structures were checked by X-ray diffraction (XRD) analysis using a Bruker AXS D8 Advance diffractometer which was run at 20–60 kV and 6–80 mA, $2\theta = 10\text{--}90^\circ$ and a step of 0.002° using $\text{CuK}\alpha$ X-ray.

The decay time, excitation and emission spectra of the phosphors were recorded by a Perkin Elmer LS 45 model luminescence spectrophotometer with xenon lamp.

Scanning electron microscopy (SEM) images and EDX analysis were performed on a LEO 440 model scanning electron microscope using an accelerating voltage 20 kV.

3. Results and discussion

Four different phosphor samples were investigated in this paper: the Mn single doped and undoped, Mn/La and Mn/Ho co-doped samples. Fig. 1 illustrates the TG/DTA curves of nominal composition for $\text{MgAl}_2\text{Si}_2\text{O}_8$. The curves before 200 °C include the dehydration of $4\text{MgCO}_3 \cdot \text{Mg}(\text{OH})_2 \cdot 5\text{H}_2\text{O}$ and the decomposition of H_3BO_3 which changes into B_2O_3 . The first endothermic peak is (at 240 °C, point A) attributed to the deviation of the hydroxyl group from $\text{Mg}(\text{OH})_2$. The second endothermic peak shows (at 437 °C, point B) the decomposition of MgCO_3 which changes into MgO .

From the above TG/DTA analysis, we carried out the sintering of the phosphors in two steps: first, the samples were pre-fired at 900 °C for 3 h to achieve the dehydration and decomposition of H_3BO_3 , MgCO_3 and $\text{Mg}(\text{OH})_2$, to help the doped Mn^{4+} and rare-earth ions to substitute; next the phosphors were prepared at 1300 °C for 3 h in air. Actually, the crystal systems were not observed at 900 °C, but

* Corresponding author. Tel.: +90 505 5075910; fax: +90 352 4374933.

E-mail address: nozpozan@erciyes.edu.tr (N.O. Kalaycioglu).

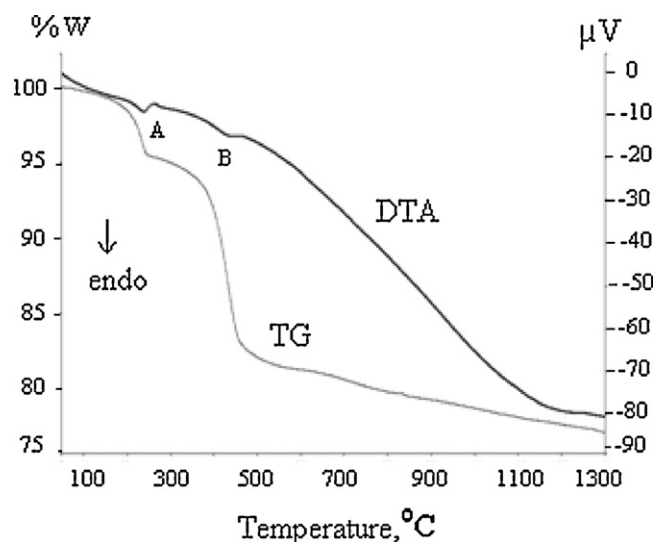


Fig. 1. TG/DTA curves of $\text{MgAl}_2\text{Si}_2\text{O}_8$ phosphor.

at 1300°C for 3 h the $\text{MgAl}_2\text{Si}_2\text{O}_8$, $(\text{Mg}_{0.90}\text{Mn}_{0.10})\text{Al}_2\text{Si}_2\text{O}_8$, $(\text{Mg}_{0.88}\text{Mn}_{0.10}\text{La}_{0.02})\text{Al}_2\text{Si}_2\text{O}_8$ and $(\text{Mg}_{0.88}\text{Mn}_{0.10}\text{Ho}_{0.02})\text{Al}_2\text{Si}_2\text{O}_8$ triclinic crystal systems were seen to have formed (Fig. 2).

The XRD patterns of phosphors obtained at 900°C and 1300°C for 3 h in air are shown in Fig. 2a–d. The unit cell parameters of phosphor crystallized in the triclinic system are listed Table 1.

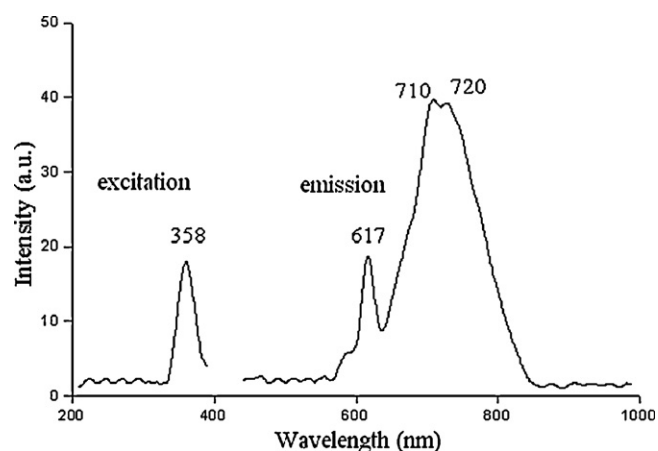


Fig. 3. The excitation and emission spectra of $\text{MgAl}_2\text{Si}_2\text{O}_8$ phosphor.

The excitation and emission spectra of undoped $\text{MgAl}_2\text{Si}_2\text{O}_8$ phosphor at room temperature are shown in Fig. 3. The excitation spectrum, monitored at 358 nm, and the emission spectrum show a broad band which can be resolved into multiple components. This broad band can be separated with maxima at about 617 nm, 710 nm and 720 nm. This red emission, with a lifetime of 2.26 ms, demonstrates that crystal defects occurred in undoped $\text{MgAl}_2\text{Si}_2\text{O}_8$ during the solid state process, because, the crystal defects in the $\text{MgAl}_2\text{Si}_2\text{O}_8$ host crystal form the basis of the luminescence center.

Fig. 4 presents the excitation and emission spectra of $(\text{Mg}_{0.90}\text{Mn}_{0.10})\text{Al}_2\text{Si}_2\text{O}_8$ phosphor under excitation at 259 nm and

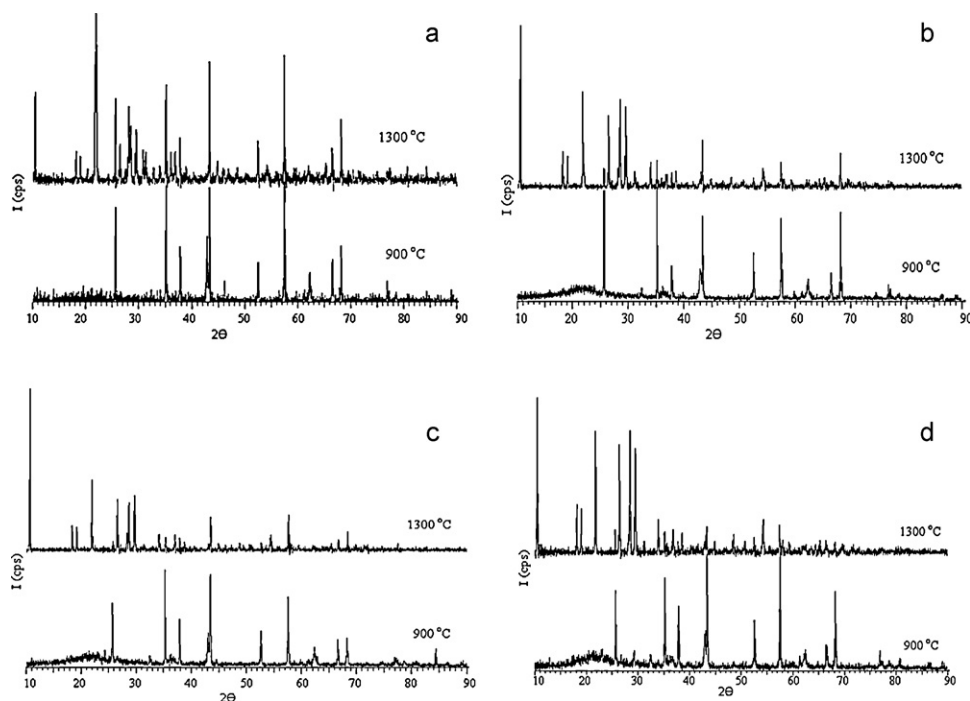


Fig. 2. XRD patterns of phosphors, (a) $\text{MgAl}_2\text{Si}_2\text{O}_8$, (b) $(\text{Mg}_{0.90}\text{Mn}_{0.10})\text{Al}_2\text{Si}_2\text{O}_8$, (c) $(\text{Mg}_{0.88}\text{Mn}_{0.10}\text{La}_{0.02})\text{Al}_2\text{Si}_2\text{O}_8$ and (d) $(\text{Mg}_{0.88}\text{Mn}_{0.10}\text{Ho}_{0.02})\text{Al}_2\text{Si}_2\text{O}_8$.

Table 1
Unit cell parameters of phosphors.

Phosphor	<i>a</i> (pm)	<i>b</i> (pm)	<i>c</i> (pm)	<i>V</i> ($\times 10^6$ pm ³)	α (°)	β (°)	γ (°)
$\text{MgAl}_2\text{Si}_2\text{O}_8$	758.28	1455.82	1472.20	940.20	46.99	84.15	77.68
$(\text{Mg}_{0.90}\text{Mn}_{0.10})\text{Al}_2\text{Si}_2\text{O}_8$	607.05	1095.86	1397.70	708.30	82.09	80.97	126.31
$(\text{Mg}_{0.88}\text{Mn}_{0.10}\text{La}_{0.02})\text{Al}_2\text{Si}_2\text{O}_8$	613.78	1305.44	1784.28	733.48	43.94	53.38	49.74
$(\text{Mg}_{0.88}\text{Mn}_{0.10}\text{Ho}_{0.02})\text{Al}_2\text{Si}_2\text{O}_8$	910.80	955.78	235.844	1781.59	87.93	78.38	116.47

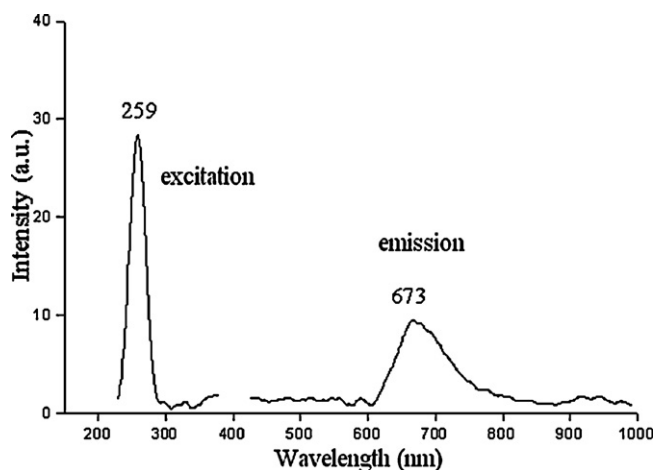


Fig. 4. The excitation and emission spectra of $(\text{Mg}_{0.90}\text{Mn}_{0.10})\text{Al}_2\text{Si}_2\text{O}_8$ phosphor.

monitored at 673 nm. Both the emission and excitation spectra were observed as broad bands at room temperature. Due to being doped with Mn^{4+} , the excitation and emission spectra of $(\text{Mg}_{0.90}\text{Mn}_{0.10})\text{Al}_2\text{Si}_2\text{O}_8$ were completely different from $\text{MgAl}_2\text{Si}_2\text{O}_8$ spectra. At less than 259 nm light excitation, the broad-band fuchsia-pink emission at 673 nm, which can be viewed as a typical emission of Mn^{4+} was ascribed to d–d transitions. The emission of Mn^{4+} at 673 nm is in good agreement with other studies [14].

The excitation at 259 nm and emission at 668 nm of $(\text{Mg}_{0.88}\text{Mn}_{0.10}\text{La}_{0.02})\text{Al}_2\text{Si}_2\text{O}_8$ phosphor are shown in Fig. 5. The typical La^{3+} emission peaks are not observed in the emission spectrum of $(\text{Mg}_{0.88}\text{Mn}_{0.10}\text{La}_{0.02})\text{Al}_2\text{Si}_2\text{O}_8$ phosphor, this indicates that La^{3+} does not act as the luminescent center in the $\text{MgAl}_2\text{Si}_2\text{O}_8$ host lattice. However, $(\text{Mg}_{0.88}\text{Mn}_{0.10}\text{La}_{0.02})\text{Al}_2\text{Si}_2\text{O}_8$ showed similar luminescent intensity as that of $(\text{Mg}_{0.90}\text{Mn}_{0.10})\text{Al}_2\text{Si}_2\text{O}_8$ phosphor UV illumination.

The excitation and emission spectra of $(\text{Mg}_{0.88}\text{Mn}_{0.10}\text{Ho}_{0.02})\text{Al}_2\text{Si}_2\text{O}_8$ phosphor are shown in Fig. 6. When the phosphor excited at 258 nm, two emission peaks, located around 679 nm and 713 nm, were observed on the emission spectrum. Such a broad fuchsia-pink emission at 679 nm can be viewed as the typical emission of d–d transitions of Mn^{4+} . The second emission peak, located around 713 nm, concerns undoped $\text{MgAl}_2\text{Si}_2\text{O}_8$. Typical Ho^{3+} emission peaks are not observed in the emission spectrum of $(\text{Mg}_{0.88}\text{Mn}_{0.10}\text{Ho}_{0.02})\text{Al}_2\text{Si}_2\text{O}_8$ phosphor. However, due to the role of Ho^{3+} ions in the luminescence

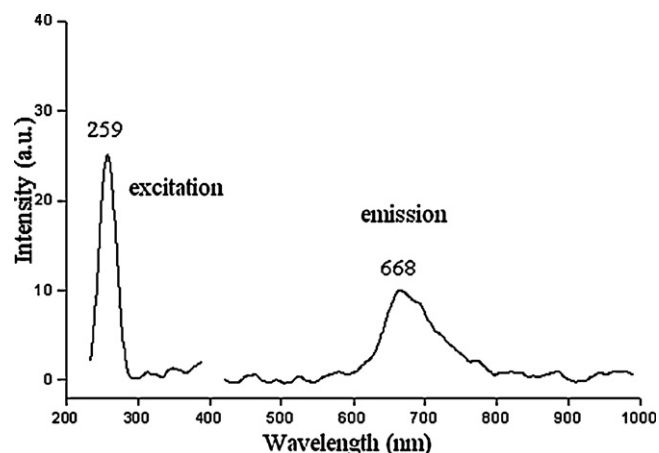


Fig. 5. The excitation and emission spectra of $(\text{Mg}_{0.88}\text{Mn}_{0.10}\text{La}_{0.02})\text{Al}_2\text{Si}_2\text{O}_8$ phosphor.

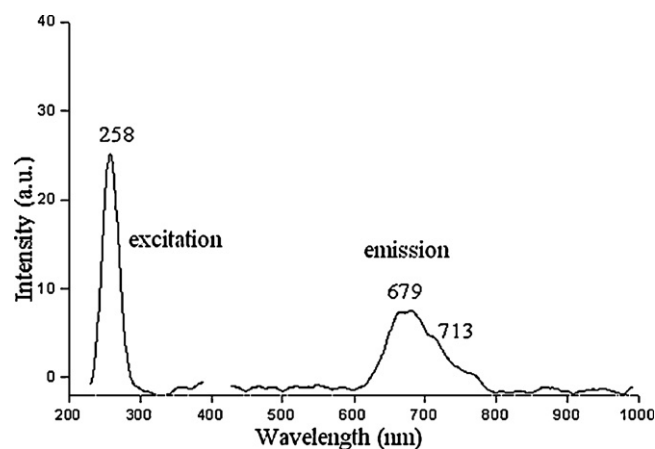


Fig. 6. The excitation and emission spectra of $(\text{Mg}_{0.88}\text{Mn}_{0.10}\text{Ho}_{0.02})\text{Al}_2\text{Si}_2\text{O}_8$ phosphor.

process, the lifetime of this phosphor, 11.20 ms, was longer than both undoped $\text{MgAl}_2\text{Si}_2\text{O}_8$ and $(\text{Mg}_{0.88}\text{Mn}_{0.10}\text{Ho}_{0.02})\text{Al}_2\text{Si}_2\text{O}_8$ phosphors.

The decay curves of the undoped $\text{MgAl}_2\text{Si}_2\text{O}_8$ and $\text{MgAl}_2\text{Si}_2\text{O}_8:\text{Mn}^{4+}$, Ho^{3+} phosphors are shown in Fig. 7a and

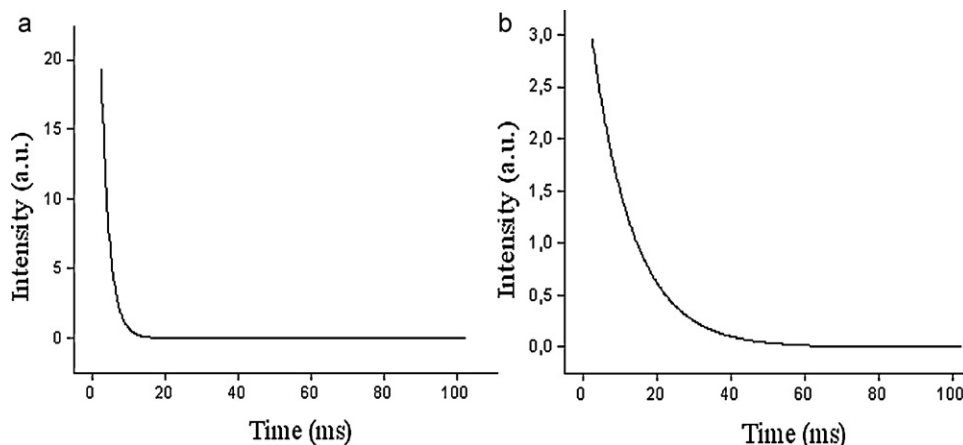


Fig. 7. The decay curves of the (a) undoped $\text{MgAl}_2\text{Si}_2\text{O}_8$ and (b) $(\text{Mg}_{0.88}\text{Mn}_{0.10}\text{Ho}_{0.02})\text{Al}_2\text{Si}_2\text{O}_8$ phosphors.

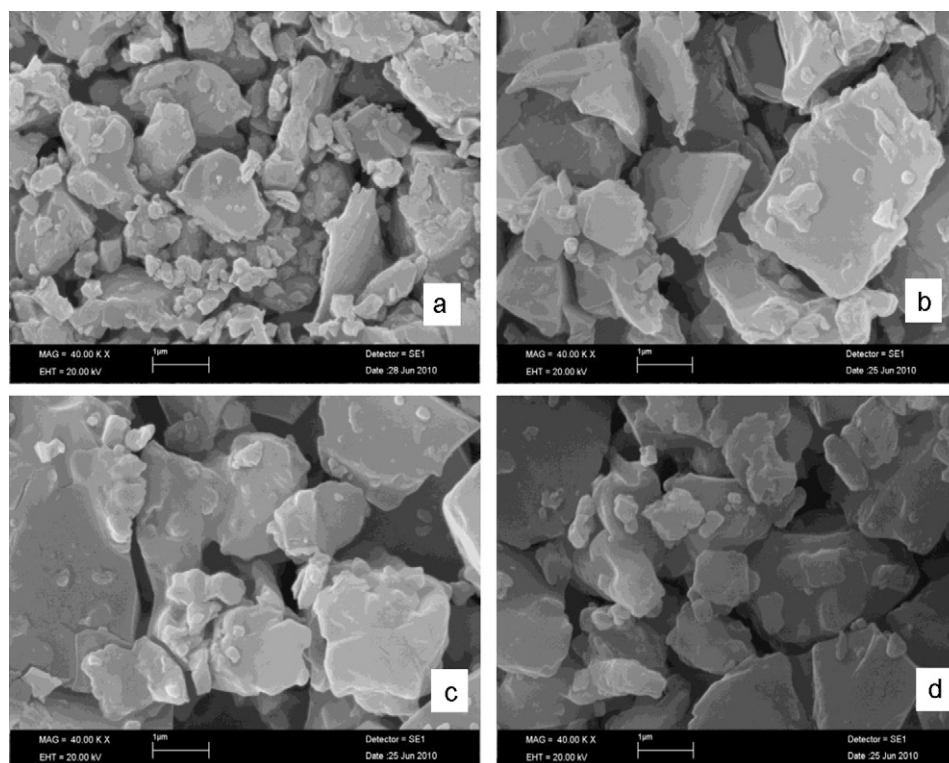


Fig. 8. SEM image of (a) $\text{MgAl}_2\text{Si}_2\text{O}_8$ phosphor, (b) $(\text{Mg}_{0.90}\text{Mn}_{0.10})\text{Al}_2\text{Si}_2\text{O}_8$ phosphor, (c) $(\text{Mg}_{0.88}\text{Mn}_{0.10}\text{La}_{0.02})\text{Al}_2\text{Si}_2\text{O}_8$ phosphor and (d) $(\text{Mg}_{0.88}\text{Mn}_{0.10}\text{Ho}_{0.02})\text{Al}_2\text{Si}_2\text{O}_8$ phosphor.

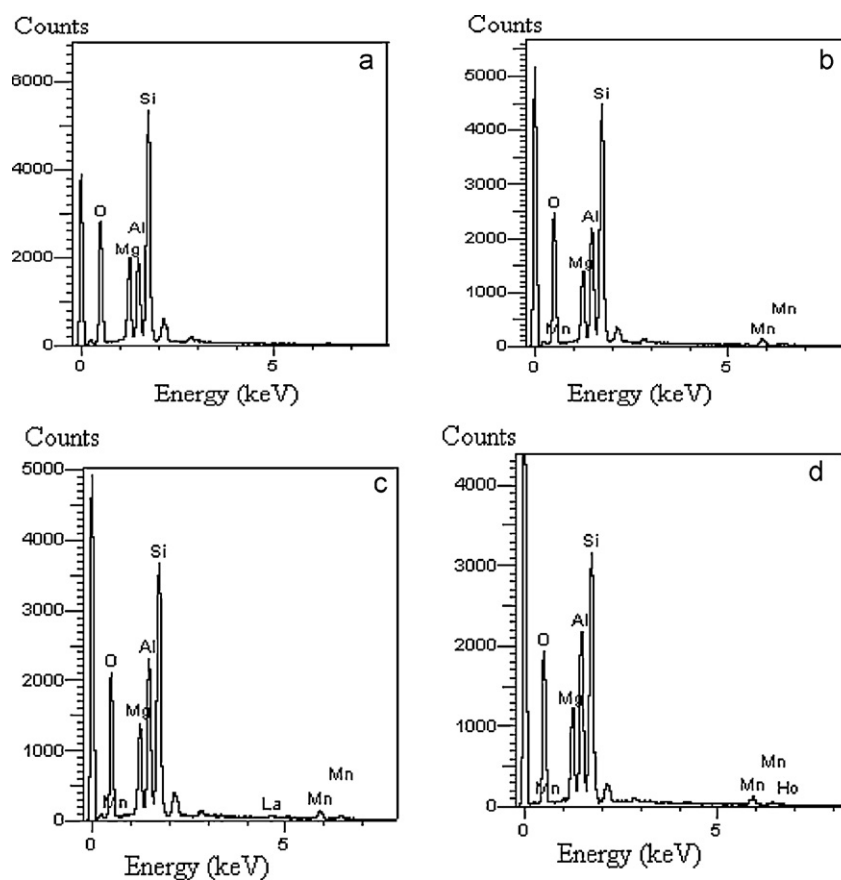


Fig. 9. EDX analysis of (a) $\text{MgAl}_2\text{Si}_2\text{O}_8$ phosphor, (b) $(\text{Mg}_{0.90}\text{Mn}_{0.10})\text{Al}_2\text{Si}_2\text{O}_8$ phosphor, (c) $(\text{Mg}_{0.88}\text{Mn}_{0.10}\text{La}_{0.02})\text{Al}_2\text{Si}_2\text{O}_8$ phosphor and (d) $(\text{Mg}_{0.88}\text{Mn}_{0.10}\text{Ho}_{0.02})\text{Al}_2\text{Si}_2\text{O}_8$ phosphor.

Table 2
Decay times for exponential components of $\text{MgAl}_2\text{Si}_2\text{O}_8$ and $(\text{Mg}_{0.88}\text{Mn}_{0.10}\text{Ho}_{0.02})\text{Al}_2\text{Si}_2\text{O}_8$ phosphors.

Phosphor	Intensity (a.u)	Decay time, τ_1 (ms)
$\text{MgAl}_2\text{Si}_2\text{O}_8$	19.30	2.26
$(\text{Mg}_{0.88}\text{Mn}_{0.10}\text{Ho}_{0.02})\text{Al}_2\text{Si}_2\text{O}_8$	2.95	11.20

b. Decay times can be calculated by a curve fitting method based on the following single exponential equation:

$$I = A_1 \exp\left(\frac{-t}{\tau_1}\right) + C$$

where I is phosphorescence intensity; A_1 , C are constants; t is time; and τ_1 is the lifetime for the exponential components. The fitting results are shown in Table 2. The Ho^{3+} co-doped phosphor shows much longer afterglow than the undoped phosphor which indicates that Ho^{3+} ions play an important role in prolonging the afterglow.

The decay times of $(\text{Mg}_{0.90}\text{Mn}_{0.10})\text{Al}_2\text{Si}_2\text{O}_8$ and $(\text{Mg}_{0.88}\text{Mn}_{0.10}\text{La}_{0.02})\text{Al}_2\text{Si}_2\text{O}_8$ phosphors cannot be detected and calculated in the same conditions.

Figs. 8 and 9 show the images and EDX analysis obtained from the scanning electron microscopy (SEM) of the phosphors calcined at 1300°C for 3 h by using solid state reactions. The microstructures of the phosphor consisted of regular fine grains with an average size of about 0.5–2.5 μm .

4. Conclusion

In this report, undoped $\text{MgAl}_2\text{Si}_2\text{O}_8$ red, $(\text{Mg}_{0.90}\text{Mn}_{0.10})\text{Al}_2\text{Si}_2\text{O}_8$, $(\text{Mg}_{0.88}\text{Mn}_{0.10}\text{La}_{0.02})\text{Al}_2\text{Si}_2\text{O}_8$ and

$(\text{Mg}_{0.88}\text{Mn}_{0.10}\text{Ho}_{0.02})\text{Al}_2\text{Si}_2\text{O}_8$ fuchsia-pink phosphors were firstly observed by using the solid state reaction at 1300°C for 3 h. The phosphors had a triclinic crystal system. The Ho^{3+} ions co-doped phosphor showed a much longer lifetime than then other phosphors.

Acknowledgement

This work was supported by Erciyes University EUBAP under Project number of FBD-09-804.

References

- [1] Y. Lin, Z. Tang, Z. Zhang, C. Nan, J. Alloys Compd. 348 (2003) 76.
- [2] Y. Wang, Z. Wang, P. Zhang, Z. Hong, X. Fan, G. Qian, Mater. Lett. 5 (2004) 3308.
- [3] C.K. Chang, D.L. Mao, Thin Solid Films 460 (2004) 48.
- [4] G. Blasse, W.L. Wanmaker, J.W. ter Vrugt, A. Bril, Philips Res. Rep. 23 (1968) 189.
- [5] T.L. Barry, J. Electrochem. Soc. 115 (1968) 733.
- [6] T.L. Barry, J. Electrochem. Soc. 115 (1968) 1181.
- [7] P.B. Moore, T. Araki, Am. Miner. 57 (1972) 1355.
- [8] K. Yamazaki, H. Nakabayashi, Y. Kotera, A. Ueno, J. Electrochem. Soc. 133 (1986) 657.
- [9] S.H.M. Poort, H.M. Reijnhoudt, G. Blasse, J. Alloys Compd. 241 (1996) 75.
- [10] L. Huang, X. Zhang, X. Liu, J. Alloys Compd. 305 (2000) 14.
- [11] S. Ye, Z. Liu, X. Wang, J. Wang, L. Wang, X. Jing, J. Lumin. 129 (2009) 50.
- [12] F. Clabau, A. Garcia, P. Bonville, D. Ganbeau, T. Mercier, P. Deniard, et al., J. Solid State Chem. 181 (2008) 1456.
- [13] Y. Ding, Y. Zhang, Z. Wang, W. Li, D. Mao, H. Han, et al., J. Lumin. 129 (2009) 294.
- [14] F. Donegan, T.J. Glynn, G.F. Imbusch, J.P. Remeika, J. Lumin. 36 (1986) 93.